

Improving Mapper’s Robustness by Varying Resolution According to Lens-Space Density

Kaleb D. Ruscitti

*Department of Pure Mathematics
University of Waterloo
Waterloo, ON, Canada*

KALEB.RUSCITTI@UWATERLOO.CA

Leland McInnes

*Tutte Institute for Mathematics and Computing
Government of Canada
Ottawa, ON, Canada*

LELAND.MCINNES@GMAIL.COM

Abstract

We propose an improvement to the Mapper algorithm that removes the assumption of a single resolution scale across semantic space, and improves the robustness of the results under change of parameters. This eases parameter selection, especially for datasets with highly variable local density in the Morse function f used for Mapper. This is achieved by incorporating this density into the choice of cover for Mapper. Furthermore, we prove that for covers with some natural hypotheses, the graph output by Mapper still converges in bottleneck distance to the Reeb graph of the Rips complex of the data, but captures more topological features than when using the usual Mapper cover. Finally, we discuss implementation details, and include the results of computational experiments. We also provide an accompanying reference implementation.

1 Introduction

It is common in data science to have a large, finite set $\mathbb{X}_n = \{x_1, \dots, x_n\}$ of samples in \mathbb{R}^d , perhaps after vectorizing real-world data. Examples include neural network embeddings of images or textual documents and single-cell RNA expression data. Given such a set, it is useful to extract the topology of the dataset, or of a topological space X from which we assume the points are sampled. One well-studied technique for doing this is *Mapper*, which uses a choice of Morse-type function f to construct a graph, or more generally, a simplicial complex, representing X (Singh et al., 2007). Mapper has many benefits; it is conceptually simple, yet is also mathematically proven to converge to the Reeb graph $R_f(X)$ in bottleneck distance asymptotically (Carriere et al., 2018). It produces finite graphs, which are computationally convenient to work with, and can be visualised in 2 dimensions even if \mathbb{X}_n lives in higher dimensions.

Unfortunately, Mapper is sensitive to the choice of initial parameters, in particular the *resolution* $r > 0$, which determines the scale of topological features which Mapper can detect. One wants to take $r \rightarrow 0$ to capture all the features of the dataset, but this would require infinitely many samples. In practice, there is a minimum r which can be chosen for a given set \mathbb{X}_n , and it is difficult to determine what that minimum is a priori. Thus, any improvements to Mapper which can make it more robust to changing r will make the algorithm more reliable for real-world data analysis.

In Mapper, the resolution is a global parameter that is fixed across the entire sample set \mathbb{X}_n . However, the range of permissible values depends on the density of the samples in the image space of the Morse-type function chosen. This density varies locally, so by making a global choice of r we are imposing a trade-off between accuracy in the dense areas, and robustness in the sparse areas. In this article, we propose a solution to this by generalising Mapper to allow

for a locally-varying choice of resolution. Furthermore, we aim to ease the choice of parameters by proposing a method for computing this variation from the data.

There is previous research which aims to improve Mapper’s parameter robustness by incorporating density. *MultiMapper* (Deb et al., 2018) has a similar idea of varying the resolution parameter locally across the sample set according to local density, but instead of changing the cover of X , they change the cover of $f(X)$. This differs from our approach in that their resolution varies only in the value of the Morse function, meaning the number of degrees of freedom is equal to the dimension of L . In our approach, we vary the resolution in all directions of \mathbb{R}^d , so even for 1-dimensional Mapper we are able to vary in d dimensions, getting a more robust cover of X . A different approach is the F - and G -Mapper proposals, which focus on improving Mapper by making a better choice of open cover with fixed r (Alvarado et al., 2023)(Bui et al., 2020). Applying G -Mapper to select an optimal initial r , and then using our work to perturb r locally, seems like a promising combination approach to arriving at a more robust Mapper algorithm.

In Section 2, we explain how to generalise Mapper using *kerneled covers*, and introduce variable-density kerneled covers to overcome the challenges above. Then, in Section 3 we cover some details of the reference implementation of our proposed algorithm. In Section 4, we show that the convergence results for Mapper generalise to kerneled covers with only minor modifications. Finally, in Section 5 we provide the results of some computational experiments.

2 Density-Based Mapper

Let \mathbb{X}_n be samples taken from some (unknown) distribution on a topological space X , with known pairwise distances, and with a choice of Morse-type function $f : X \rightarrow \mathbb{R}$. In this section, we will assume some knowledge of the theory of Morse-type functions. For a good introduction to the Morse theory used here, the reader is referred to Section 2 of Carrière and Oudot (2018).

2.1 Kernel Perspective on Mapper

Let $\mathcal{U} = \{U_i\}_{i=1}^N$ be a finite open cover of $f(\mathbb{X}_n)$, and define the corresponding *pullback cover* of \mathbb{X}_n to be $\mathcal{V} = \{f^{-1}(U_i)\}_{i=1}^N$. Then the Mapper graph associated to (X, f, \mathcal{U}) is defined to be the nerve $N(\mathcal{V})$. More concretely, we choose a clustering algorithm, cluster each set $f^{-1}(U_i)$, and label the clusters $\{v^i_j\}_{j=1}^{J_i}$. Then the Mapper (weighted) graph G has vertices given by

$$V(G) := \bigcup_{i=1}^N \{v^i_j\}_{j=1}^{J_i},$$

and edges

$$E(G) = \bigcup_{i=1}^{N-1} \{(v^i_j, v^{i+1}_{j'}) \mid j \in J_i, j' \in J_{i+1}\},$$

with weight on the edge $(v^i_j, v^{i+1}_{j'})$ given by $\#\{x \in \mathbb{X}_n \mid x \in v^i_j \cap v^{i+1}_{j'}\}$. To generalize this, we will rewrite the sets $f^{-1}(U_i)$. Let $\chi_i : \mathbb{R} \rightarrow \{0, 1\}$ be the characteristic function of U_i ,

$$\chi_i(t) = \begin{cases} 1, & t \in U_i, \\ 0, & t \notin U_i. \end{cases}$$

Then, we can rewrite:

$$f^{-1}(U_i) = f^{-1}(\chi_i^{-1}(1)). \tag{1}$$

Moreover, if U_i is an open interval with midpoint $m_i \in \mathbb{R}$ and width w , so that

$$U_i = \left(m_i - \frac{w}{2}, m_i + \frac{w}{2}\right),$$

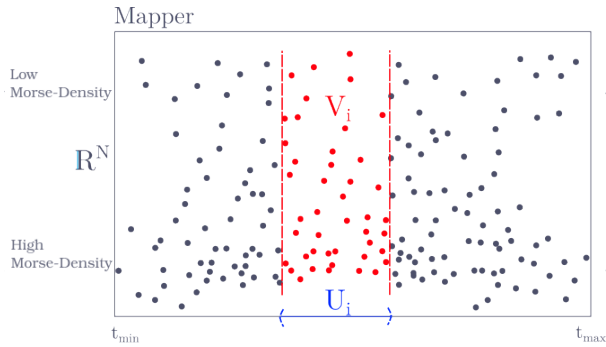


Figure 1: Pullback open set $f^{-1}(U_i)$ of the interval U_i , in red.

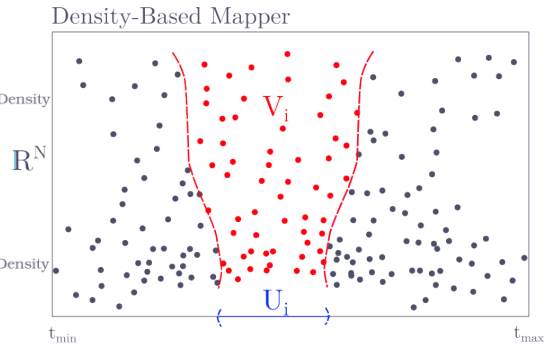


Figure 2: Density-sensitive kernel set corresponding to U_i

then Equation 1 tells us $f^{-1}(U_i)$ is the result of applying a square window function of width w , centered at m_i , to \mathbb{X}_n . Explicitly, let $K_i(x) : \mathbb{X}_n \rightarrow \mathbb{R}$ be

$$K_i(x) := \begin{cases} 1, & |f(x) - m_i| < w/2, \\ 0, & \text{otherwise.} \end{cases}$$

Then $f^{-1}(U_i) = K_i^{-1}(1)$. This suggests one approach to generalize Mapper. By defining new kernel functions, one obtains new covers \mathcal{V} to take the nerve of. As long as the kernel satisfies certain width hypotheses, the statistical guarantees of Mapper can be preserved.

2.2 Density-Sensitive Kerneled Covers

Now, to construct a Mapper which is sensitive to the density information of \mathbb{X}_n , we will replace the pullback cover with a *kerneled cover*, using a kernel function that takes local density as one of its arguments. To obtain a cover of X , we require that the kernels chosen have *sufficient width*.

Definition 1 (*f*-kernel, sufficient width) An *f*-kernel function $K : X \times \mathbb{R} \rightarrow \mathbb{R}$ centered at $t_0 \in L$ is a function such that:

1. If $f(x) = t_0$ then $K(x, t_0) = 1$.
2. K is continuous on the set $\{x \in X \mid K(x, \rho) > 0\} \subset X$.
3. For a fixed t_0 , $K(x, t_0)$ is monotone non-increasing in $|f(x) - t_0|$.

For a fixed $r > 0$, we say that a choice of kernel K and $\epsilon > 0$ has sufficient width if $|f(x) - t_0| < r \implies K(x, t_0) > \epsilon$.

Let \mathcal{U} be a generic open maximal interval cover, or *gomic* of $L = [t_{\min}, t_{\max}] \subset \mathbb{R}$, by which we mean a cover of open intervals where no more than two intervals intersect at a time and such that the *overlap g* between U_i and U_j , defined by

$$g := \frac{\ell(U_i \cap U_j)}{\ell(U_i)}, \quad \text{where } \ell \text{ is Lebesgue measure,}$$

satisfies $g \in (0, 1)$, for all i, j with $U_i \cap U_j \neq \emptyset$ (Carrière and Oudot, 2018, §2.5). Let N be the number of intervals in \mathcal{U} . For each U_i in \mathcal{U} , fix a midpoint m_i . We say a family of kernel functions $\{K_i\}_{i=1}^N$ has sufficient width relative to \mathcal{U} for threshold $\epsilon > 0$, if K_i centered at m_i has sufficient width with radius $r = \ell(U_i)/2$, for every $U_i \in \mathcal{U}$.

Definition 2 Given (X, f) , \mathcal{U} and $\{K_i\}_{i=1}^N$ as above, the kerneled cover of X associated to (\mathcal{U}, K) , with threshold $\epsilon > 0$, is the cover \mathcal{V} consisting of sets

$$V_i := K_i^{-1}(\epsilon, \infty)$$

for every $i = 1, \dots, N$.

The sufficient width condition guarantees that the kernels are wide enough to ensure that \mathcal{V} covers the entire space X .

Proposition 3 Let \mathcal{U} be an open cover of \mathbb{R}^n consisting of open balls $B(r_i, t_i)$. Let \mathcal{V} be the kerneled cover for (\mathcal{U}, K) with threshold ϵ . If the $\{K_i\}$ have sufficient width relative to \mathcal{U} , then \mathcal{V} is an open cover of X .

Proof The set $V_i \in \mathcal{V}$ is defined as $V_i = K^{-1}(\epsilon, \infty)$, and so by continuity of K , V_i is open. Moreover, the sufficient width condition of (K, ϵ_i) tells you that $f^{-1}(U_i) \subset V_i$ as follows: If $x \in f^{-1}(U_i)$ then $|f(x) - t_0| < r_i$ and hence by sufficient width, $K(x, f(x)) > \epsilon$. Now because $\{U_i\}$ is a cover, $\mathcal{V} = \{f^{-1}(U_i)\}$ is a cover, and thus

$$X \subset \bigcup_{i \in I} f^{-1}(U_i) \subset \bigcup_{i \in I} V_i.$$

■

Next, we want to determine a scaling factor for the width of the kernel function, which varies with the *lens space density* of the dataset. Let $\beta(x)$ be the distance in L from x to its k th nearest neighbour in X . Then we need to choose a continuous function $c(\beta) : [0, \infty) \rightarrow [1, c_{\max}]$.

Although any such choice is reasonable, in the reference implementation we chose a normalized sigmoid function:

$$c(\beta) = c_{\max} \left(1 + \exp \left[\frac{-(\beta - \mu)}{\sigma} \right] \right),$$

where μ, σ are the mean and standard deviation of $\beta(x)$ respectively. This choice was made because this function is approximately linear within a standard deviation of the mean of $\beta(x)$, meaning the width of the kernel will be most sensitive in the range of β where most of the data lies. However, the function is still bounded on both sides, allowing us to control the maximum and minimum width of the kernel.

Finally, one has to normalize the chosen kernel function to guarantee sufficient width. For example, if we are using a Gaussian kernel, $K(x, t_0) \propto \exp(c(\beta)(f(x) - t_0)^2)$, we can solve for a normalization constant which ensures $K(x, t_0)$ has sufficient width:

Proposition 4 Suppose $K(x, t_0) = \exp \left[\frac{2 \log(\epsilon)}{r^2} c(\beta) \frac{(f(x) - t_0)^2}{2} \right]$ is the kernel function associated to the open ball $B(r, t_0)$. Then $K(x, t_0)$ has sufficient width for threshold ϵ .

Proof Suppose x_0 is such that $|f(x) - t_0| < r$. Using this inequality and the inequality $c(\beta) \geq 1$, we have:

$$\begin{aligned} K(x_0, t_0) &= \exp \left[\frac{2 \log(\epsilon)}{r^2} c(\beta) \frac{(f(x_0) - t_0)^2}{2} \right] \\ &> \exp \left[\frac{2 \log(\epsilon)}{r^2} \frac{r^2}{2} \right] \\ &= \epsilon. \end{aligned}$$

■

For any other choice of kernel function, such as those used in kernel density estimation, a similar process can be used to determine a normalization constant which guarantees sufficient width.

Remark 5 *You can always use a square kernel to obtain the same kerneled cover as you would obtain with any non-square kernel. Thus, if you are not using the value of $K(x, t)$ as a weight for the edges of the Mapper graph, or as a weight for the clustering algorithm, then there is no benefit to using a non-square kernel.*

Later on, we will need a generalization of the resolution parameter of Mapper:

Definition 6 *Let \mathcal{V} be an open cover of a manifold X , with Morse-type function $f : X \rightarrow L \subset \mathbb{R}$. Let the resolution of \mathcal{V} be*

$$r := \sup_{v \in V} \left(\sup_{x, y \in V} |f(x) - f(y)| \right).$$

When \mathcal{V} is the pullback under f of an open cover \mathcal{U} for L , this reduces to the resolution for regular Mapper, $r = \sup_{U \in \mathcal{U}} \ell(U)$.

3 Implementation

Let $\mathbb{X}_n \subset \mathbb{R}^d$ be a set of samples, and let $\{t_1, \dots, t_n\}$ denote the associated values of f . Fix a clustering algorithm CA, and four parameters; $k, N \in \mathbb{N}$, $g \in (0, 1)$ and an f -kernel function K . A high-level overview of the proposed algorithm is:

Algorithm Density-based Mapper

Input: $(\mathbb{X}_n, \{t_1, \dots, t_n\})$ as above, with parameters N, g, k and K .

Output: A weighted graph G .

1. Compute the inverse (approximate) *Morse density* $\beta(x)$ for $x \in \mathbb{X}_n$.
2. Determine an open cover of intervals $\mathcal{U} = \{U_i = B(w_i, t_i)\}_{i=1}^N$ that have overlap g .
3. For each interval U_i ,
 - 3.a Compute the kernel $K(x, t_i)$ for each $x \in \mathbb{X}_n$, and define $V_i = \{x \mid K(x, t_i) > \epsilon\}$.
 - 3.b Run the clustering algorithm CA to assign each point in V_i a cluster label $c_i(x) \in \{c_i^1, \dots, c_i^{J_i}\}$.
 - 3.c Add vertices $\{c_i^1, \dots, c_i^{J_i}\}$ to $V(G)$.
4. For $i = 1, \dots, n - 1$,
 - 4.a Compute the intersection $I_i = V_i \cap V_{i+1}$,
 - 4.b For each point $x_i \in I_i$, add weight $K(x, t_i)$ to the edge between $c_i(x)$ and $c_{i+1}(x)$.

Return $G = (V(G), E(G))$.

In the following sections, we will elaborate on steps 1 and 2. There is also a reference implementation available on GitHub:

<https://github.com/tutteinstitute/temporal-mapper>

3.1 Approximating the Morse Density

To approximate the Morse density of X at a point x , we want to choose an appropriate open set U around x , and then compute the density of $f(U)$. As the open sets get large, the Morse density becomes more blurred across the dataset. If the open sets get too small relative to the density of the data, there is not enough samples in the open set to get an accurate approximation. As is typical in situations where one wants to find open sets whose size varies with the density of the data, we use k nearest neighbour distance to define our open sets. Once we have an open set, the density of $f(U)$ will be $k/\ell(f(U))$, which we call the approximate Morse density of x . However to avoid division-by-zero problems, we implement everything in terms of the *inverse* approximate Morse density. In summary:

Algorithm

Input: $(\mathbb{X}_n, \{t_1, \dots, t_n\})$, and a parameter $k \in \mathbb{N}$.

Output: For each $x \in \mathbb{X}_n$, a value $\beta(x) \in \mathbb{R}$.

1. For each $x_i \in \mathbb{X}_n$, find the set of k nearest neighbours, $\{x_{i_1}, \dots, x_{i_k}\}$. Let $J_i := \{i_1, \dots, i_k\}$
2. For each $x_i \in \mathbb{X}_n$, define:

$$\tilde{\beta}(x) = \max_{i_j \in J_i} (t_{i_j}) - \min_{i_j \in J_i} (t_{i_j}).$$

3. Smooth $\tilde{\beta}(x)$ by convolving with a window function $W(x, y)$;

$$\beta(x) := \frac{1}{n} \sum_{y \in \mathbb{X}_n} \tilde{\beta}(y) W(x, y).$$

The reference implementation uses a cosine window for the last step, with width

$$w^{(d)} = \left(\max_{x \in \mathbb{X}_n} x^{(d)} - \min_{x \in \mathbb{X}_n} x^{(d)} \right) / 10,$$

where $v^{(d)}$ denotes the d th component of the vector v .

3.2 Selecting Intervals for the Open Cover

To perform Mapper, we must choose an open cover of the lens space. In particular, we want to construct a generic open minimal interval cover, or *gomic*; see (Carrière and Oudot, 2018, §2.5). There are multiple natural ways to select a gomic for the lens space $L = [t_{\min}, t_{\max}]$. Fix a number N of open intervals, and an overlap parameter g . For any open interval $(a, b) = I_i \subset \mathbb{R}$, let the midpoint be $t_i := (b - a)/2$. One choice is to take open intervals with fixed length; $\ell(I_i) = \ell(I_j)$ for all $i, j \in \{1, \dots, N\}$. In this case, the midpoints of the intervals will be evenly spaced in L , so we will call this method *Morse-spaced* cover selection.

Definition 7 Let $L = [t_{\min}, t_{\max}]$, and fix $N \in \mathbb{N}$ and $g \in [0, 1]$. Let $\Delta = (t_{\max} - t_{\min})/N$ and $t_i := t_{\min} + i\Delta$, for each $i \in \{1, \dots, n\}$. The Morse-spaced cover with parameters (N, g) is the open cover $\mathcal{U} = \{I_1, \dots, I_N\}$ of L defined by:

$$I_i = \left(t_i - \frac{\Delta}{2} \left(1 + \frac{g}{2} \right), \quad t_i + \frac{\Delta}{2} \left(1 + \frac{g}{2} \right) \right) \cap L.$$

The Morse-spaced cover has the advantage of producing graphs whose vertices are evenly spaced in L and are therefore very interpretable in terms of f . However, for datasets where the amount of samples are not very evenly distributed in L , the Morse-spaced cover will have a highly variable number of points in each interval. This can make it difficult to select parameters for the clustering algorithm CA used in Mapper. For these datasets, we can make a mild interpretability sacrifice to mitigate this issue by choosing the intervals such that the number of datapoints in each set is the same; we called this *data-spaced* cover selection.

Definition 8 Fix $N \in \mathbb{N}$ and $g \in [0, 1]$. Let $t_k = f(x_k)$, for $x_k \in \mathbb{X}_n$. Sorting if necessary, suppose $t_k \leq t_{k+1}$ for all $k \in \{1, \dots, k\}$. Let $j_i = 1 + \left\lceil \frac{i(n-1)}{N} \right\rceil$, for all $i \in \{0, \dots, N\}$. Then the data-spaced cover with parameters (N, g) is the open cover $\mathcal{U} = \{I_1, \dots, I_N\}$ of L defined by:

$$I_i = \left(t_{j_{i-1}} \left(1 - \frac{g}{2} \right), t_{j_i} \left(1 + \frac{g}{2} \right) \right).$$

Remark 9 The data-spaced cover can fail to be an open cover when there exists an i such that $t_{j_{i-1}} = t_{j_i}$. This can happen if N is very large or if there exists one region with extremely high Morse-space density.

Now given the set $\mathcal{U} = \{U_i\}$, we can define the kerneled pullback cover of X associated to \mathcal{U} and K : $\mathcal{V} = \{V_i\}_{i=1}^N$ where

$$V_i = \{x \in X \mid K(x, t_i) > \epsilon\}.$$

3.3 Parameter Selection

When applying density-based Mapper to a dataset, one must make a choice of parameters r, g, k and K . In this section, we will provide some heuristic rules to help practitioners choose reasonable values for these parameters.

The parameter which is most influential on the output graph is the resolution r , or if using the reference implementation, $N \sim 1/r$. In the reference implementation, this is the required `N_checkpoints` parameter. In subsection 4.5 we show that the resolution determines which topological features we will be able to see in the output, and for this reason we want to make N large. On the other hand, if N is too large, we run into a limit imposed by the number of data points; some slices will have too few points to get good clustering and cluster overlaps. When the Morse function f has a natural interpretation, such as time, one can use an apriori understanding of the dataset to choose a reasonable N .

Remark 10 In the reference implementation, `N_checkpoints` determines the minimum resolution of the kerneled cover, so it is better to take N a little bit larger than you would do with standard Mapper.

In addition to choosing N , the resolution is also affected by the choice of Morse-spaced or data-spaced intervals. Whenever your data is approximately equally spaced in L , you should select Morse-spaced intervals. However, if there are some L -ranges with unusually high or low volumes of data, then you may have trouble getting clusters in those regions that are consistent with the rest of the dataset. This can cause artifacts in the resulting graph. To avoid this, you can use data-spaced intervals.

The last parameter that determines the cover of the lens space \mathcal{U} is the overlap parameter g . In the reference implementation, this is the parameter `overlap`, which is scaled to lie within $(0, 1)$. As with N , g determines the *minimum* overlap between intervals, so consider taking a

smaller g than you would with regular Mapper. In our experimentation, we find that the output graphs are fairly robust under changing g . A reasonable default choice is $g = 0.5$.

Next, we have the parameter k , which is the number of nearest neighbours used in the density computation. Increasing k smooths out the inverse Morse density $\beta(x)$. Moreover, the choice of k is very influential on the runtime of the reference implementation; computing the k -nn graph is the slowest operation in density-based Mapper. For this reason, you want to take k as small as you can get away with. Unfortunately, as you reduce k , the value of $\beta(x)$ becomes more and more sensitive to small changes in the relative position of the embedded samples x_i . This means that for low k , the results of the Mapper become less robust to changes in representation of the samples in \mathbb{R}^d . For datasets with 100k-1M points, we have empirically found that $100 \leq k \leq 250$ seems to be reasonable.

Finally, there is the choice of the kernel K . The simplest choice is to use square kernels, with width varying as a function of β . When your clustering algorithm of choice does not support passing weights for the points, any other kernel is equivalent to a square kernel. However, if you are using a clustering algorithm that can take weights for the points, such as `scikit-learn.cluster.DBSCAN`, then the values of $K(x, t)$ can be used as weights for the points to get more refined clusters. In the reference implementation, the Gaussian kernel from Proposition 4 is available as an alternative to the square kernel.

Using the reference implementation, one can recover standard Mapper by choosing a square kernel, and setting the `rate_sensitivity` parameter equal to 0. This will skip the density computation, and the square kernel K_i will be equal to the characteristic function of U_i , for every interval in the cover \mathcal{U} .

4 Convergence to the Reeb Graph

One reason to use Mapper is that there are theoretical results about its convergence to the Reeb graph as the resolution goes to zero. Here we prove that this property is preserved by our proposed changes. In this section, we use connected to mean path connected.

4.1 Persistence Diagrams and Bottleneck Distance

First, we recall the definition of zig-zag homology, persistence diagrams, and the bottleneck distance, following (Carrière and Oudot, 2018, §2.2-2.3). Let f be Morse type on a topological space X , such as a graph. Let $X^{(a)}$ be the sublevel set $X^{(a)} := f^{-1}(-\infty, a]$. Then the family $\{X^{(a)}\}_{a \in \mathbb{R}}$ defines a filtration, meaning $X^{(a)} \subseteq X^{(b)}$ for $a \leq b$. Of course, if we reverse the interval, letting $X_{op}^{(b)} = f^{-1}[b, \infty)$, we get an opposite filtration; we index these by $b \in \mathbb{R}_{op}$. These filtrations can be ‘connected at infinity’ as follows. Replace $X_{op}^{(b)}$ by the pair of spaces $(X, X_{op}^{(b)})$, and define $\mathbb{R}_{\text{Ext}} = \mathbb{R} \cup \{\infty\} \cup \mathbb{R}_{op}$, with order $a < \infty < \tilde{a}$ for all $a \in \mathbb{R}$ and $\tilde{a} \in \mathbb{R}_{op}$, and define the extended filtration to be

$$X_{\text{Ext}}^{(a)} := \begin{cases} f^{-1}(-\infty, a], & a \in \mathbb{R} \\ X & a = \infty, . \\ (X, f^{-1}[a, \infty)), & a \in \mathbb{R}_{op} \end{cases}$$

Taking homology of this filtration defines the *extended persistence module* $\text{EP}(f)$. If the critical values of f are $\{-\infty, a_1, a_2, \dots, a_n, +\infty\}$, then $\text{EP}(f)$ is the sequence

$$0 \rightarrow H_* \left(X^{(a_0)} \right) \rightarrow \dots \rightarrow H_* \left(X^{(a_n)} \right) \rightarrow H_*(X) \rightarrow H_* \left(X_{\text{Ext}}^{(a_n)} \right) \rightarrow \dots \rightarrow H_* \left(X_{\text{Ext}}^{(a_0)} \right) \rightarrow 0.$$

When f is Morse type, the extended persistence module decomposes into interval modules:

$$\text{EP}(f) = \bigoplus_{k=1}^n \mathbb{I}[b_k, d_k),$$

where $\mathbb{I}[b_k, d_k) = (\mathbb{R} \times [b_k, d_k)) \cup (\{0\} \times \mathbb{R}_{\text{Ext}} - [b_k, d_k))$. Each summand represents the lifespan of a ‘homological feature’, such as a connected component or non-contractible loop. The endpoints b_k and d_k are called the *birth time* and *death time* of the feature. This structure can be represented by plotting the points (b_k, d_k) in \mathbb{R}^2 , and this plot is called the *extended persistence diagram* of (X, f) denoted $\text{Dg}(X, f)$.

Next, we will define a pseudometric on persistence diagrams, called the bottleneck distance. First, we need the concept of a matching:

Definition 11 *A partial matching between persistence diagrams D and D' is a subset Γ of $D \times D'$ such that if $(p, p') \in \Gamma$ and $(p, q') \in \Gamma$ then $p' = q'$, and the same for (p, p') and (q, p') . Furthermore, if $(p, p') \in \Gamma$, then the type (ordinary, relative, extended) of p and p' must match.*

Let $\Delta \subset \mathbb{R}^2$ be the diagonal. The cost of Γ is

$$\text{cost}(\Gamma) := \max \left\{ \max_{p \in D} \delta_D(p), \max_{p' \in D'} \delta_{D'}(p') \right\},$$

where $\delta_D(p) = \|p - p'\|_\infty$ if $(p, p') \in \Gamma$ or $\delta_D(p) = \inf_{q \in \Delta} \|p - q\|_\infty$ otherwise.

Definition 12 (Bottleneck distance) *The bottleneck distance between D and D' is*

$$d_\Delta(D, D') := \inf_{\Gamma} \text{cost}(\Gamma),$$

ranging over all partial matchings Γ of D and D' .

We call $\delta_D(p)$ the transport cost of p . Note that if $p = (b, d)$ then

$$\inf_{q \in \Delta} \|p - q\|_\infty \leq \inf_{q \in \Delta} \|p - q\|_2 = |b - d|.$$

If $\delta_D(p) > \inf_{q \in \Delta} \|p - q\|_\infty$, then we can modify Γ by removing (p, p') to get a partial matching with lower cost. Therefore, when computing the bottleneck distance between D and D' we know it is bounded above by $\max_{(b,d) \in D \cup D'} |b - d|$.

Proposition 13 *Suppose X is a topological space and that $f : X \rightarrow \mathbb{R}$ is a Morse function. Then the endpoints of a persistence interval $[b, d)$ of $\text{EP}(f)$ only occur at critical values of f .*

Proof Suppose that $b \in \mathbb{R}_{\text{Ext}}$, and there is no critical point x with $f(x) = b$. Let t_0 be the largest critical value of f less than b . Then, because f is Morse-type and there are no critical points in the interval (t_0, b) , $X^{(b)}$ deformation retracts onto $X^{(t_0)}$. Then because $X^{(b)}$ deformation retracts to $X^{(t_0)}$, they must have isomorphic homology groups, and thus b cannot be the endpoint of a persistence interval. By the contrapositive, the endpoints of persistence intervals occur only at the critical values of f . ■

Zigzag persistence modules are a generalization of persistence modules, where one permits some of the arrows in the sequence to go backwards (Carlsson and de Silva, 2008). In particular, we want to make use of the *levelset zigzag persistence module*.

Definition 14 Let $f : X \rightarrow \mathbb{R}$ be Morse type, and let its critical values be labeled $\{a_1, \dots, a_n\}$. Pick any set of values $\{s_i\}_{i=1}^n$ such that $a_i < s_i < a_{i+1}$, where $a_0 = -\infty, a_{n+1} = \infty$. Let $X_i^j = f^{-1}([s_i, s_j])$. Then the levelset zigzag persistence module $\text{LZZ}(X, f)$ is the sequence:

$$H_* (X_0^0) \rightarrow H_* (X_0^1) \leftarrow H_* (X_1^1) \rightarrow H_* (X_1^2) \leftarrow \dots \rightarrow H_* (X_{n-1}^n) \leftarrow H_* (X_n^n),$$

with linear maps induced by inclusions of the topological spaces.

As with the extended persistence module, the levelset zigzag module decomposes into a sum of intervals, and the disjoint union of all those intervals is called the levelset zigzag persistence barcode, denoted $\text{LZZ}_{bc}(X, f)$.

Proposition 15 For X a topological space with Morse type function f , there exists a bijection between $\text{Dg}(X, f)$ and $\text{LZZ}_{bc}(X, f)$.

Proof Corollary of the Pyramid Theorem in [Carlsson et al. \(2009\)](#). ■

It is through the levelset zigzag that we will relate the persistence diagrams of Mapper and the Reeb graph.

4.2 Mapper Graphs from Zigzag Modules

Let X be a topological space with a Morse function $f : X \rightarrow \mathbb{R}$. Suppose $\mathcal{V} = V_{i=1}^N$ is a cover of X . Then we can form the zig-zag module

$$\begin{array}{ccccc} H_0(V_1) & & H_0(V_2) & & H_0(V_N) \\ & \swarrow \phi_{1,2}^1 & \nearrow \phi_{1,2}^2 & \swarrow \phi_{N-1,N}^{N-1} & \nearrow \phi_{N-1,N}^N \\ & H_0(V_1 \cap V_2) & & \dots & \end{array}$$

The Mapper graph associated to this cover \mathcal{V} is a combinatorial graph representation of this zig-zag module. For each of the ‘upper’ vector spaces, that is, those of the form $H_0(V_i)$, we choose a basis $\{v_j^i\}_{j=1}^{J_i}$ of the connected components of V_i . For each of the ‘lower’ vector spaces, those of the form $H_0(V_i \cap V_{i+1})$, we choose a basis $\{e_k^{i,i+1}\}_{k=1}^{K_i}$.

Definition 16 The multinerve Mapper graph \bar{G} associated to the zig-zag module (4.2) is a multigraph defined by vertex set

$$V(G) = \bigcup_{i=1}^N \{v_1^i, \dots, v_{J_i}^i\},$$

and edge set

$$E(G) = \bigcup_{i=1}^{N-1} \left\{ \left(\phi_{i,i+1}^i(e_k^{i,i+1}), \phi_{i,i+1}^{i+1}(e_k^{i,i+1}) \right), k = 1, \dots, K_i \right\}$$

The Mapper graph G is the graph obtained from \bar{G} by identifying all the parallel edges into single edges. Standard Mapper refers to the Mapper graph G associated to the pullback cover $f^{-1}(\mathcal{U}) = \{f^{-1}(U_i) \mid U_i \in \mathcal{U}\}$ of a gomic \mathcal{U} .

For point cloud data, we can form a discrete approximation of this graph. Let \mathbb{X}_n be a set of samples taken from a space $X \subset \mathbb{R}^d$. Let $f : X \rightarrow \mathbb{R}$ be a Morse-type function, and let $\text{Rips}_\delta(\mathbb{X}_n)$ denote the Rips complex of \mathbb{X}_n with radius δ . Recall that *single-linkage* clustering is a clustering algorithm for samples \mathbb{X}_n in which the clusters are the connected components of $\text{Rips}_\delta(\mathbb{X}_n)$. Replacing X with $\text{Rips}_\delta(\mathbb{X}_n)$ and forming the (multinerve) Mapper graph yields the

discrete (multinerve) Mapper graph. More generally, one can replace single-linkage clustering with an arbitrary clustering algorithm, and then replace connected components of the sets V_i with clusters.

We let $M_{\mathcal{U},\delta}(\mathbb{X}_n, f)$ denote the discrete Mapper graph constructed with the cover $f^{-1}(\mathcal{U})$ and single-linkage clustering. That is, the graph with vertices given by

$$V(G) := \bigcup_{U_i \in \mathcal{U}} \left\{ \text{connected components of } \text{Rips}_\delta \left(f^{-1}(U_i) \right) \right\},$$

and edges given by adding an edge between two vertices for each $x \in \mathbb{X}_n \cap (U_i \cap U_j)$ which is in both connected components.

For any continuous manifold and Morse function X, f , the continuous Mapper graph with respect to the cover $f^{-1}(\mathcal{U})$ is denoted $M_{\mathcal{U}}(X, f)$. The continuous multinerve Mapper graph is denoted $\bar{M}_{\mathcal{U}}(X, f)$. If $\{K_i\}_{U_i \in \mathcal{U}}$ are kernels defining the kerneled cover \mathcal{V} associated to \mathcal{U} , then the density-based continuous Mapper graph will be denoted $M_{\mathcal{U},K}(X, f)$, and the density-based continuous multinerve Mapper graph will be denoted $\bar{M}_{\mathcal{U},K}(X, f)$.

Furthermore, these graphs are themselves topological spaces, and we can define a Morse-type function on them derived from f . For any open set $V \subset \mathbb{R}^d$, define the midpoint m_V to be

$$m_V := \min_{x \in V} (f(x)) + \left[\max_{x \in V} f(x) - \min_{x \in V} f(x) \right] / 2.$$

When $I \subset \mathbb{R}$ is an interval and $V = f^{-1}(I)$, m_V agrees with the midpoint of the interval I . Let G denote any of the Mapper graphs above. By the definition of Mapper, any vertex $v \in V(G)$ is associated to an open set $V \subset X$. Therefore, we can define $\bar{f} : V(G) \rightarrow \mathbb{R}$ by $V \rightarrow m_V$, and extend it to a function $\bar{f} : G \rightarrow \mathbb{R}$ piecewise linearly.

One advantage of Mapper is that the graphs it produces converge in bottleneck distance to the Reeb graph in the asymptotic limit, $n \rightarrow \infty$. Any modifications made to the algorithm should aim to preserve this property; here we verify that the density-based changes we made preserve this limit. In this section, we must make use of the algebraic machinery of zigzag persistence. For a concise introduction to the theory used here one can look at (Carrière and Oudot, 2018, §2). Here we will only recall the critical definitions and results, without proof.

To prove the convergence of density-based Mapper, we follow the proof of the convergence for Mapper: (Carriere et al., 2018, Theorem 2.7). There, the proof is broken into lemmas, which we now modify for density-based Mapper. One key idea is to construct a specific zigzag persistence module, called the *cover zigzag persistence module* (Carrière and Oudot, 2018, Def. 4.4) which relates the persistence diagram of the Reeb graph $R_f(X)$ and the Mapper graph $M_{\mathcal{U}}(X, f)$. The proof generalizes to kerneled covers after defining the correct *kerneled cover zigzag persistence module* to generalize the cover zigzag persistence module.

4.3 Kerneled Cover Zigzag Persistence

Everywhere in this section, let $f : X \rightarrow L \subset \mathbb{R}$ be Morse-type, with critical values $\{-\infty = a_0, a_1, \dots, a_{n+1} = +\infty\}$, indexed in increasing order, and let $\mathcal{U} = \{I_i\}_{i=1}^N$ be a gomic of L . Suppose each value a_i corresponds to a unique critical point x_{c_i} .

To prove the bottleneck distance convergence for Mapper, Carriere and Oudot define the *cover zigzag persistence module*, whose barcode encodes the persistence diagram of Mapper. First we recall their definition, and then we generalize it to kerneled covers.

Definition 17 (Carrière and Oudot, 2018, Def. 4.4) *For any open interval I with left endpoint a , we define the integers $l(I)$ and $r(I)$ by*

$$l(I) = \max\{i : a_i \leq a\} \qquad r(I) = \max(l(I), \max\{i : a_i \in I\}).$$

Then we define the cover zigzag persistence module $\text{CZZ}(f, \mathcal{U})$ by

$$H_* \left(X_{l(I_1)}^{r(I_1)} \right) \leftarrow \cdots \rightarrow H_* \left(X_{l(I_k)}^{r(I_k)} \right) \leftarrow H_* \left(X_{l(I_k \cap I_{k+1})}^{r(I_k \cap I_{k+1})} \right) \rightarrow H_* \left(X_{l(I_{k+1})}^{r(I_{k+1})} \right) \leftarrow \cdots \rightarrow H_* \left(X_{l(I_N)}^{r(I_N)} \right)$$

Proposition 18 (*Carrière and Oudot, 2018, Lemma 4.5*) *With $f : X \rightarrow L$, and open cover \mathcal{U} as above, there is a bijection between $\text{Dg}(\bar{M}_{\mathcal{U}}, \bar{f})$ and $\text{CZZ}_{bc,0}(f, \mathcal{U})$.*

We generalize:

Definition 19 *Let $\mathcal{U} = \{U_i\}_{i \in [N]}$ be a gomic of L , and let $\mathcal{V} = \{V_i\}_{i \in [n]}$ be a kerneled cover of X associated to \mathcal{U} . The kerneled cover zigzag persistence module $\text{KCZZ}(f, \mathcal{V})$ is*

$$H_*(V_1) \leftarrow \cdots \rightarrow H_*(V_k) \leftarrow H_*(V_k \cap V_{k+1}) \rightarrow H_*(V_{k+1}) \leftarrow \cdots \rightarrow H_*(V_N)$$

Remark 20 *If a set V_k does not contain a critical point of f , then there is a deformation retract onto the previous set V_{k-1} . This gives an isomorphism:*

$$H_*(V_{k-1}) \cong H_*(V_{k-1} \cap V_k) \cong H_*(V_k).$$

In the remainder of this section, we will assume that we've reduced the kerneled cover zigzag persistence module by removing all such isomorphic terms. In particular, we assume therefore that each V_k contains a critical point of f .

For a square kernel, where \mathcal{V} is the pullback cover, this is isomorphic to the cover zigzag persistence module $\text{CZZ}(f, \mathcal{U})$.

Proposition 21 *Let X be a topological space with Morse-function f , and covers \mathcal{U} and \mathcal{V} as in the definition above. Then $\text{LZZ}_0(\bar{M}_{\mathcal{U},K}, \bar{f})$ and $\text{KCZZ}(f, \mathcal{V})$ are equal as zigzag persistence modules.*

Proof

Let m be the number of critical points of $(\bar{M}_{\mathcal{U},K}, \bar{f})$, so that $\text{LZZ}_0(\bar{M}_{\mathcal{U},K}, \bar{f})$ contains $2m + 1$ terms. By the definition of \bar{f} , these can occur only at vertices of $\bar{M}_{\mathcal{U},K}$, which are connected components of open sets in \mathcal{V} . Therefore, if \bar{f} has a critical point at a vertex v_j^i inside set V_i , then V_i contains a critical point of f . This implies that there are at least m many V_i containing critical points, and therefore $\text{KCZZ}(f, \mathcal{V})$ has at least $2m + 1$ terms.

However, some of these terms will be isomorphic. Suppose that V_i contains a critical point which is inside a connected component v_j^i , but that v_j^i is not a critical point of f . Then this implies that there exists a deformation retract of $\bar{M}_{\mathcal{U},K}$ to the previous critical point of \bar{f} , ordered in terms of \bar{f} , say v^k . This deformation retract induces an isomorphism $H_*(V_k) \cdot H_*(V_k) \cdots \cong H_*(V_i)$ for $k \leq \cdots \leq i$. If $k = i$ then V_i is one of the m sets counted above, and otherwise it is isomorphic to one. Therefore the number of non-isomorphic terms in $\text{KCZZ}(f, \mathcal{V})$ is $2m + 1$. Now it remains to show that the $2m + 1$ terms of $\text{KCZZ}(f, \mathcal{V})$ and $\text{LZZ}_0(\bar{M}_{\mathcal{U},K}, \bar{f})$ are equal.

The even terms of the zeroth dimension levelset zig-zag have the form:

$$H_0(X_i^{j+1}) = H_0 \left(\bar{f}^{-1}[s_i, s_{i+1}] \right).$$

By definition, there is one critical value of \bar{f} , a_{i+1} , in the interval $[s_i, s_{i+1}]$. Critical values of \bar{f} occur only at vertices of $\bar{M}_{\mathcal{U},K}(X, f)$; let v_i be the vertex with $\bar{f}(v_i) = a_{i+1}$. By definition of

$\bar{M}_{\mathcal{U},K}(X, f)$, v_i is a connected component of $V_{j_i} \subset X$ for some $j_i \in [N]$, and all the connected components of V_{j_i} define vertices with $\bar{f} = a_i$. Therefore:

$$\begin{aligned} \dim H_0 \left(\bar{f}^{-1}[s_i, s_{i+1}] \right) &= \#\{v \in V(\bar{M}_{\mathcal{U},K}(X, f)) \mid \bar{f}(v) = a_i\} \\ &= \#\{\text{connected components of } V_{j_i}\} \\ &= \dim H_0(V_{j_i}). \end{aligned}$$

Moreover, since $\text{KCZZ}(f, \mathcal{V})$ only includes V_k that contain a critical point, the value a_{i+1} will be associated to a vertex in V_{i+1} .

The odd terms of the levelset zig-zag have the form

$$H_0(X_i^?) = H_0 \left(\bar{f}^{-1}(s_i) \right).$$

By construction, s_i is not a critical value of \bar{f} . Suppose there is some vertex v of $\bar{M}_{\mathcal{U},K}(X, f)$ with $\bar{f}(v) = s_i$. Then v is not a critical point, and hence $\bar{f}^{-1}(s_i)$ is homotopy equivalent to $\bar{f}^{-1}(s_i - \epsilon)$, for all sufficiently small $\epsilon > 0$. Hence we can, up to replacing s_i by $s_i - \epsilon$, assume that there is no vertex with $\bar{f}(v) = s_i$. Following the argument from the even case, the critical values a_i and a_{i+1} can be associated to sets V_i and V_{i+1} in the cover \mathcal{V} . Since \bar{f} is defined by piecewise linear extension, the points in $\bar{M}_{\mathcal{U},K}(X, f)$ which have a value of s_i will lie on edges connecting vertices associated to connected components in V_i and V_{i+1} . Thus,

$$\begin{aligned} \dim H_0 \left(\bar{f}^{-1}(s_i) \right) &= \#\{\text{edges between connected components of } V_i \text{ and } V_{i+1}\} \\ &= \dim H_0(V_i \cap V_{i+1}). \end{aligned}$$

Thus each term of these two zig-zag modules are isomorphic. ■

Proposition 22 *There exists a bijection between $\text{Dg}(\bar{M}_{\mathcal{U},K}, \bar{f})$ and $\text{KCZZ}_{cb,0}(f, \mathcal{V})$.*

Proof Combine the previous result with Prop. 15. ■

4.4 Convergence of Continuous Density-Based Mapper

Recall that our goal is to relate the diagram $\text{Dg}(\bar{M}_{\mathcal{U},K}, \bar{f})$ with the persistence diagram of the Reeb graph, $\text{Dg}(R_f(X), f)$. We have related $\text{Dg}(\bar{M}_{\mathcal{U},K}, \bar{f})$ with the kerneled cover zig-zag module, and so next we must relate $\text{KCZZ}(f, \mathcal{V})$ to $\text{Dg}(R_f(X), f)$.

For standard multinerve Mapper, this relationship is given by the next theorem.

Theorem 23 *Let X be a topological space, and $f : X \rightarrow \mathbb{R}$ a Morse-type function. Let $R_f(X)$ be the Reeb graph, and by abuse of notation, $f : R_f(X) \rightarrow \mathbb{R}$ the induced map. Let \mathcal{U} be a gomic of $f(X)$, with resolution r . Then*

$$\text{Dg}(R_f(X), f) - \{(x, y) \mid |y - x| \leq r\} \subset \text{Dg}(\bar{M}_{\mathcal{U}}(X, f)) \subset \text{Dg}(R_f(X), f)$$

Proof This is the first half of Corollary 4.6 of [Carrière and Oudot \(2018\)](#). ■

Remark 24 *Theorem 23 for Multinerve Mapper reduces to Mapper as well. Consider the projection $\pi : \bar{M}_{\mathcal{U}}(X, f) \rightarrow M_{\mathcal{U}}(X, f)$ by identifying all edges connecting the same pair of vertices. For 1d Mappers, this projection induces a surjection in homology (Carrière and Oudot, 2018, Lemma 3.6). Using this, one can show*

$$\text{Dg}(R_f(X), f) - \{(x, y) \mid |y - x| \leq r\} \subset \text{Dg}(M_{\mathcal{U}}(X, f)) \subset \text{Dg}(\bar{M}_{\mathcal{U}}(X, f)) \subset \text{Dg}(R_f(X), f).$$

The same argument applies when substituting in a kerneled cover.

Given a kerneled cover \mathcal{V} associated to an open cover \mathcal{U} of L , we can define two pullback covers:

Definition 25 *Let X be a continuous manifold, $f : X \rightarrow L \subset \mathbb{R}$ a Morse-type function, and K an f -kernel of sufficient width with respect to some cover \mathcal{U} of L . Let \mathcal{V} be the cover associated to (\mathcal{U}, K) . The maximally-coarse cover \mathcal{U}^c of L associated to this data is the set consisting of*

$$U_i^c := \left(\inf_{x \in V_i} f(x), \sup_{y \in V_i} f(x) \right)$$

for all $V_i \in \mathcal{V}$, and we let \mathcal{V}^c denote its pullback cover of X . Analogously, the maximally-fine cover \mathcal{U}^f of L associated to this data is the set consisting of

$$U_i^f := \left(\sup_{x \in V_i} f(x), \inf_{y \in V_i} f(x) \right)$$

for all $V_i \in \mathcal{V}$, and we let \mathcal{V}^f denote its pullback cover of X .

Definition 26 *Let X be a topological space with Morse-function $f : X \rightarrow \mathbb{R}$. Here we call a finite open cover $\mathcal{V} = \{V_i\}_{i=1}^N$ of X regular, if*

1. *For all $1 \leq i \leq N$, $\ell(V_i \cap V_{i+1}) > 0$, where ℓ denotes Lebesgue measure.*
2. *For all $i \neq j \neq k$, $V_i \cap V_j \cap V_k = \emptyset$.*
3. *\mathcal{V} has no proper subcovers.*

This is engineered so that the maximally coarse and fine covers \mathcal{U}^c and \mathcal{U}^f associated to \mathcal{V} will be gomics.

Then, for $f : X \rightarrow L$, with a choice of \mathcal{U} and K , we have three covers of X , $\mathcal{V}, \mathcal{V}^f$ and \mathcal{V}^c , which define three continuous Mappers of X , which we denote $M_{\mathcal{U}, K}(X, f)$, $M_{\mathcal{U}}^f(X, f)$ and $M_{\mathcal{U}}^c(X, f)$. Let r_f and r_c denote the resolution of \mathcal{V}^f and \mathcal{V}^c respectively.

Proposition 27 *Suppose that $\mathcal{V} = \{V_i\}$ and $\tilde{\mathcal{V}} = \{\tilde{V}_i\}$ are two regular covers of L with the same number of sets, and that $V_i \subset \tilde{V}_i$ for every i . Then the number of path connected components of \tilde{V}_i is less than or equal to the number of path connected components of V_i for every i .*

Proof Let C be a path connected component of \tilde{V}_i . Then either $C \cap V_i$ is connected, or it has connected components C_1, \dots, C_K . If C_i and D_j are connected components of \tilde{V}_i , then $C_i \cap V_i$ and $D_j \cap V_i$ must not be in the same connected component of V_i : Suppose for contradiction that they were in the same connected component E . Then there is a path γ from some point $p_c \in C_i \cap V_i$ to some point $p_d \in D_j \cap V_i$. However, since $\gamma \subset E \subset V_i \subset \tilde{V}_i$, this path would also connect C and D , contradicting the hypothesis. ■

In particular, for any kerneled cover \mathcal{V} , we have that $V_i^f \subset V_i \subset V_i^c$ for all i .

Definition 28 Suppose that $\mathcal{V} = \{V_i\}$ and $\tilde{\mathcal{V}} = \{\tilde{V}_i\}$ are two regular covers of L with the same number of sets, and that $V_i \subset \tilde{V}_i$ for every i . Then the coarse-node identification map $\phi : M_{\mathcal{U},K}(X, f) \rightarrow M_{\mathcal{U}}(X, f)$ is the graph morphism defined as follows. Any vertex $v \in M_{\mathcal{U},K}(x, f)$ is a connected component of an open set $V_i \in \mathcal{V}$. There is a corresponding $\tilde{V}_i \supset V_i$ whose connected components are the vertices of $M_{\mathcal{U}}(X, f)$. Let $\phi(v)$ be the connected component of v in \tilde{V}_i . If $e = (u, v)$ is an edge of $M_{\mathcal{U},K}(X, f)$, then let $\phi(e) = (\phi(u), \phi(v))$.

Proposition 29 The coarse-node identification map ϕ is well-defined and surjective.

Proof

First, for well-definedness, let $e = (v_1, v_2)$ be an edge of M_K . Then there exists a point $x \in v_1 \cap v_2 \subset V_i \cap V_{i+1}$. As $v_1 \subset \phi(v_1)$ and $v_2 \subset \phi(v_2)$, we have $x \in \phi(v_1) \cap \phi(v_2)$ and thus the edge $\phi(e)$ exists in M , hence ϕ is well defined. Next we prove that ϕ is surjective.

Suppose $a \in \mathbb{R}$ is a critical value of f . Then, because $V_i \subset \tilde{V}_i$, the number of connected components of \tilde{V}_i is less than or equal to the number of connected components of V_i . Therefore, the number of vertices of the graph M associated to a is less than or equal to the number of vertices of the graph M_K associated to a . Therefore, at each such value, the map $\phi : V_a(M_K) \rightarrow V_a(M)$ by taking a connected component in V_i to its connected component in \tilde{V}_i is surjective.

Suppose $e = (w_1, w_2)$ is an edge of M . Then there exists a point y in $w_1 \cap w_2 \subset \tilde{V}_i \cap \tilde{V}_{i+1}$. It is possible that $y \notin V_i \cap V_{i+1}$, but since \mathcal{V} is a cover, either $y \in V_i$ or $y \in V_{i+1}$. WLOG, suppose $y \in V_i$. Then let v_1 be the connected component of y in V_i , and let v_2 be $v_1 \cap V_{i+1}$. It remains to show that $v_2 \neq \emptyset$.

Since $y \in w_1 \cap w_2$, we have that $w_1 \cap w_2 \neq \emptyset$ and thus w_1 and w_2 belong to the same connected component C inside $\tilde{V}_i \cup \tilde{V}_{i+1}$. Let $A = V_i \cap C$ and $B = V_{i+1} \cap C$. Then $A \cup B = C$, $A \cap w_1 = v_1$ and $B \cap w_2 = v_2$. Furthermore $A \cap B = V_i \cap V_{i+1} \cap C = v_1 \cap V_{i+1} = v_2$. Therefore if $v_2 = \emptyset$, then A and B would disconnect C , a contradiction. \blacksquare

The coarse-node identification map between the maximally coarse Mapper and density-based Mapper can be interpreted as a map of modules from $KCZZ(f, \mathcal{V}) \rightarrow CZZ(f, U^c)$, as we now explain. The slice $f^{-1}(I_i)$ is homotopy equivalent to $X_{l(I_i)}^{r(I_i)}$ for every $I_i \in U^c$, and thus $H_0(X_{l(I_i)}^{r(I_i)})$ is generated by the connected components of $f^{-1}(I_i)$, which are vertices $\{v_j^i\}$ of the coarse Mapper. On the other hand, $H_0(V_i)$ is generated by the connected components of V_i , which are vertices of the density-based Mapper, which surject via ϕ onto $H_0(X_{l(I_i)}^{r(I_i)})$.

Thus, we have the following:

$$\text{Dg}(\bar{M}_{\mathcal{U}}, \bar{f})^c \subset \text{KCZZ}_{cb,0}(f, \mathcal{V}) \subset \text{Dg}(\bar{M}_{\mathcal{U}}, \bar{f})^f.$$

Combining Equation 4.4, Theorem 23 and Proposition 22, we can now obtain the convergence result for continuous density based Mapper.

Theorem 30 Let X be a topological space, and $f : X \rightarrow \mathbb{R}$ a Morse-type function. Let $R_f(X)$ be the Reeb graph, and let \mathcal{V} be a cover of X with maximally coarse resolution r . Then

$$\text{Dg}(R_f(X), f) - \{(x, y) \mid |y - x| \leq r\} \subset \text{Dg}(\bar{M}_{\mathcal{U},K}(X, f), \bar{f}) \subset \text{Dg}(R_f(X), f).$$

Moreover, the persistence diagrams become equal if r is smaller than the smallest difference between distinct critical values of f .

Proposition 31 Let \mathcal{V} be a kernal cover of (X, f) associated to (\mathcal{U}, K) and let $\tilde{\mathcal{U}}$ be the associated maximally-coarse cover. Then

$$d_{\Delta} \left(\text{Dg}(R_f(X)), \text{Dg}(M_{\mathcal{U},K}, \bar{f}) \right) \leq r,$$

where r is the resolution of $\tilde{\mathcal{U}}$.

Proof This is a corollary of the inclusion result above. ■

4.5 Convergence of Discrete Density-Based Mapper

Now that we know density-based Mapper converges to the Reeb graph when we have access to a bona fide continuous manifold X , it remains to understand what happens when we work with samples $\mathbb{X}_n \leftarrow X$.

First, we generalize a result about the Mapper of the the Rips-complex to kerneled covers from [Dey and Wang \(2013\)](#).

Definition 32 Let $G = (\mathbb{X}_n, E)$ be a graph with vertices \mathbb{X}_n . For $e = (x, x') \in E$, let $I(e)$ be the interval

$$(\min(f(x), f(x')), \max(f(x), f(x'))).$$

Then e is said to be intersection-crossing for the gomic \mathcal{U} if there is a pair of consecutive intervals $U_i, U_j \in \mathcal{U}$ such that $U_i \cap U_j \subset I(e)$.

Proposition 33 Let $\text{Rips}_\delta^1(\mathbb{X}_n)$ denote the 1-skeleton of $\text{Rips}_\delta(\mathbb{X}_n)$. If it has no intersection-crossing edges, then $M_{\mathcal{U}, \delta, K}(\mathbb{X}_n, f)$ and $M_{r, g, K}(\text{Rips}_\delta, f)$ are isomorphic as combinatorial graphs.

Proof Let $L \subset \mathbb{R}$ denote the image of $f(X)$, and let \mathcal{U} be the open cover of L used in the density-based Mapper algorithm. For each $U_i \in \mathcal{U}$, let $K_i(x) = K(x, t_i)$ for the midpoint $t_i \in U_i$.

A vertex of $M_{r, g, K}(\text{Rips}_\delta, f)$ is a connected component of $\text{Rips}_\delta(\mathbb{X}_n) \cap V_i$, for some $V_i = K_i^{-1}(\epsilon, \infty)$. Denote these connected components as c_i^j , $j = 1, \dots, J_i$. The connected components of $\text{Rips}_\delta(\mathbb{X}_n) \cap V_i$ are the same as the connected components of its 1-skeleton, which are the vertices of $M_{\mathcal{U}, K, \delta}(\mathbb{X}_n, f)$ by definition. Therefore the set of vertices $\{c_i^j\}$ of these graphs are the same.

It remains to construct an isomorphism on the edges. An edge $(c_{i_1}^j, c_{i_2}^k)$ of $M_{\mathcal{U}, K, \delta}(\mathbb{X}_n, f)$ corresponds to a point $x \in \mathbb{X}_n$ which is in the intersection of two pullbacks; $x \in V_{i_1} \cap V_{i_2}$, and which is in the connected component $c_{i_1}^j \subset V_{i_1}$ and $c_{i_2}^k \subset V_{i_2}$. On the other hand, an edge $(c_{i_1}^j, c_{i_2}^k)$ of $M_{r, g, K}(\text{Rips}_\delta, f)$ is a point $x \in X$ with the same property. This shows the edges of $M_{\mathcal{U}, K, \delta}(\mathbb{X}_n, f)$ are a subset of the edges of $M_{r, g, K}(\text{Rips}_\delta, f)$, but we still need to check the other inclusion.

By regularity of the cover \mathcal{U} , the intersection $U_{i_1} \cap U_{i_2}$ is an interval I . The existence of an edge in $M_{r, g, K}(\text{Rips}_\delta, f)$ implies that the components $c_{i_1}^j$ and $c_{i_2}^k$ are connected in $V_{i_1} \cup V_{i_2}$; call this connected component C . Since C is connected, its 1-skeleton is connected, so there is a 1-cell \tilde{e} connecting $c_{i_1}^j$ and $c_{i_2}^k$. Let its endpoints be denoted u and v , which are both points in \mathbb{X}_n . If $f(u) \in I$, then u will define an edge in $M_{\mathcal{U}, K, \delta}(\mathbb{X}_n, f)$, and same with v . Otherwise, the edge \tilde{e} is intersection-crossing. Thus if $\text{Rips}_\delta^1(\mathbb{X}_n)$ has no intersection-crossing edges, then the set of edges of $M_{\mathcal{U}, K, \delta}(\mathbb{X}_n, f)$ and $M_{r, g, K}(\text{Rips}_\delta, f)$ are equal. ■

Using these lemmas, one can recover the convergence result:

Definition 34 (Reach and Convexity Radius) Let $X \subset \mathbb{R}^d$ be a topological space. The medial axis of X is the set of points in \mathbb{R}^d with at least two nearest neighbours in X :

$$\text{med}(X) := \left\{ y \in \mathbb{R}^d \mid \#\{x \in X \mid \|y - x\| = \|y, X\|\} \geq 2 \right\},$$

where $\|y, X\| = \inf\{\|y - x\| \mid x \in X\}$. The reach of X , rch is the distance $\inf\{\|x - m\| \mid x \in X, m \in \text{med}(X)\}$.

The convexity radius of X is the supremum of $\rho \in \mathbb{R}$ for which every ball in X of radius less than ρ is convex.

Definition 35 (Modulus of Continuity) Let $f : X \rightarrow \mathbb{R}$ be a Morse-type function. The modulus of continuity ω_f of f is the function $\mathbb{R}_{\geq 0} \rightarrow \mathbb{R}_{\geq 0}$,

$$\omega_f(\delta) = \sup\{|f(x) - f(x')| \mid x, x' \in X, \|x - x'\| \leq \delta\}$$

Theorem 36 Suppose X is a compact continuous manifold with positive reach rch and convexity radius ρ . Let $\mathbb{X}_n \leftarrow X$ be n points sampled from X . Let f be a Morse-type function on X with modulus of continuity ω . Then if the three following hypotheses hold:

1. $\delta \leq \frac{1}{4} \min\{\text{rch}, \rho\}$ and $\omega(\delta) \leq \frac{1}{2}e_{\min}$,
2. $\max\{|f(x_i) - f(x_j)| \mid x_i, x_j \in \mathbb{X}_n, \text{ such that } \|x_i - x_j\| \leq \delta\} \leq gr$,
3. $4d_H(X, \mathbb{X}_n) \leq \delta$,

Then the bottleneck distance between the density-based Mapper with single-linkage clustering and the Reeb graph satisfies

$$d_{\Delta}(R_f(X), M_{\mathcal{U}, K, \delta}(\mathbb{X}_n, f)) \leq r + 2\omega(\delta).$$

Proof The proof proceeds exactly as the proof of Theorem 2.7 in [Carriere et al. \(2018\)](#), replacing their Theorems A2 and A4 with our Propositions 33 and 31. We provide a sketch here. As shorthand, let $M_{\mathcal{U}, \delta, K} = M_{\mathcal{U}, \delta, K}(\mathbb{X}_n, f)$.

$$\begin{aligned} d_{\Delta}(R_f(X), M_{\mathcal{U}, \delta, K}) &= d_{\Delta}(\text{Dg}(R_f(X), f), \text{Dg}(M_{\mathcal{U}, \delta, K}, f)) \\ &= d_{\Delta}(\text{Dg}(R_f(X), f), \text{Dg}(M_{\mathcal{U}, K}(\text{Rips}_{\delta}(\mathbb{X}_n), \bar{f}))) \\ \text{(triangle inequality)} &\leq d_{\Delta}(\text{Dg}(R_f(X), f), \text{Dg}(R_{\bar{f}}(\text{Rips}_{\delta}(\mathbb{X}_n), \bar{f}))) \\ &\quad + d_{\Delta}(\text{Dg}(R_{\bar{f}}(\text{Rips}_{\delta}(\mathbb{X}_n), \bar{f})), \text{Dg}(M_{\mathcal{U}, K}(\text{Rips}_{\delta}(\mathbb{X}_n), \bar{f}), \bar{f})) \\ &\leq 2\omega(\delta) + r/2 \end{aligned}$$

The equality from first to second line is due to Proposition 33, which holds due to hypothesis 2), and the final equality is due to hypotheses 1) and 3), and Proposition 31. \blacksquare

Theorem 36 tells us that density-based Mapper will perform at least as well (in bottleneck distance) as regular Mapper for the same gomic \mathcal{U} . Furthermore, it allows one to apply the statistical analysis of Mapper by Carriere, Michel and Oudot ([Carriere et al., 2018, §3-4](#)) to density-based Mapper.

5 Computational Experiments

This section explains the computational experiments we used to validate density-based Mapper.

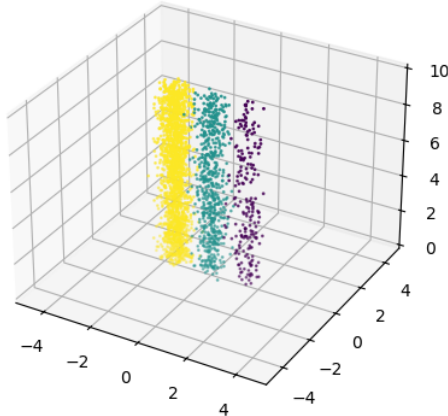


Figure 3: Synthetic data for morse density computation.

5.1 Verifying the Approximate Morse Density Computation

First, before testing density-based Mapper on any data, we will check that the proposed approximation of the Morse density is sensible. If our method works, we should be able to recreate Figure 2 experimentally.

To this end, we generated the data shown in Figure 3. For a Morse function, we used projection to the vertical axis. The data consists of three components, each with different Morse densities. The x and y directions are sampled from a circular Gaussian distribution, and the t direction is sampled from uniform random on $L = [0, 10]$. Python code used to generate this data is included in Appendix A.

Figure 4 shows this data; the y -axis is a 1 dimensional principal component of the xy -plane, and the x -axis is the value of the Morse function. In the left-hand plot, the colouration denotes the inverse Morse density. The right-hand plot denotes the pullback of the interval $I = (3.65, 3.87)$. Points between the black lines would be included in $f^{-1}(I)$, the pullback open set that Mapper would use. Points coloured red are those in $K^{-1}(0.1, \infty)$, which is the kerneled open set associated to I with threshold 0.1.

Comparing Figure 2 to Figure 4, we can see that our implementation is doing what we set out to do. In the regions where the Morse density is lower, the kerneled cover's open sets get larger, and vice-versa. Now we can proceed with tests on more complicated datasets to evaluate how these changes to the open cover effect the output of the Mapper graph.

5.2 Comparison of Mapper and Density-Based Mapper on Variable-Density data

The motivation for proposing density-based Mapper was to improve the performance of Mapper on datasets that have regions of varying Morse density. The claim is that density-based Mapper is better at detecting small features in dense regions, while preserving the correct large features in sparse regions. This experiment is intended to provide evidence for this claim with one example.

For this experiment we generated a minimal dataset which exhibits the type of topology which Mapper has a hard time correctly reconstructing: see Figure 5. There is one component which has high density and a 1-dimensional topological feature (a loop), and another component which has much lower density. With regular Mapper, the choice of resolution parameter is difficult. If the intervals in the cover \mathcal{U} are too small, the sparse component will not be captured as there is not enough points per set. If they are too wide, the genus-1 feature in the dense component will be lost. On the other hand, with density-based Mapper the relative densities

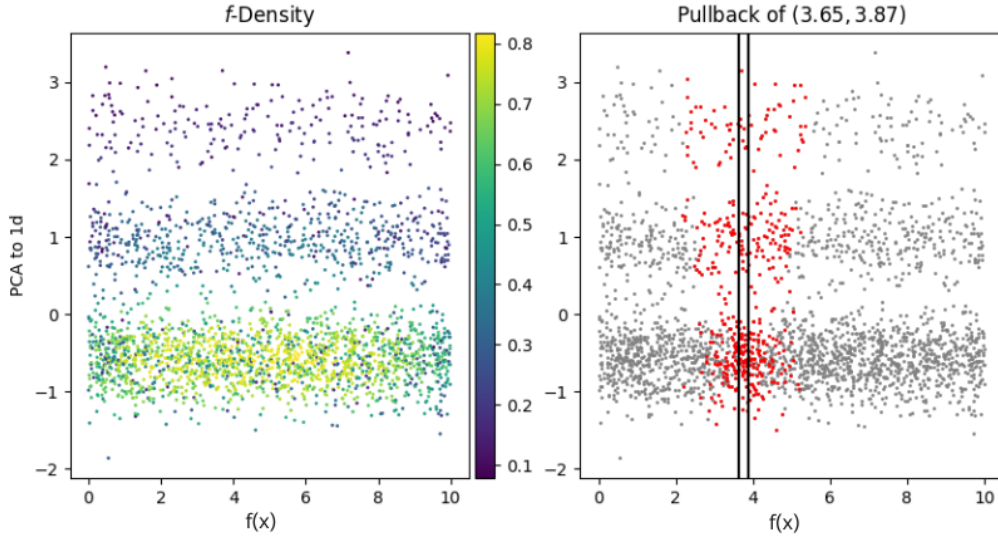


Figure 4: Left: Colour represents the Morse density. Right: Points in the kerneled pullback are red.

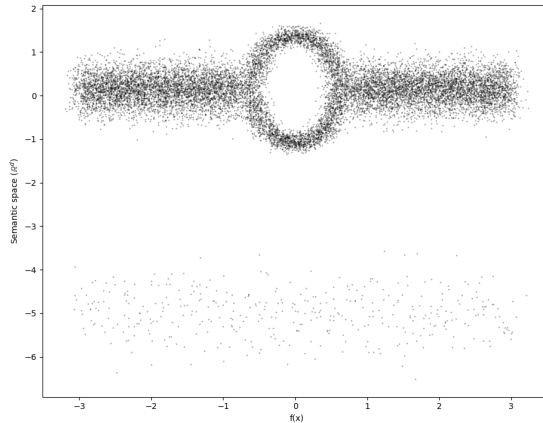


Figure 5: Synthetic data with a genus-1 component.

of the components will be factored in, widening the kerneled cover around the low density component and narrowing them around the high density component. This allows density-based Mapper to detect both the genus-1 feature and the sparse component for a much wider range of parameters than standard Mapper.

To test this, we ran both algorithms multiple times, varying the number of open sets n and their overlap g ; Figures 6 and 7 show the results for standard and density-based Mapper respectively, with the clustering algorithm DBSCAN, and the Morse-spaced cover (Def. 7). For density-based Mapper, a square kernel was used. In the plot, the vertices were positioned by using the average position of the data points in their corresponding cluster. We've added a green box around each correct output.

Standard Mapper is able to recover the topology, with some noise, in 3 out of 25 tests, whereas density-based Mapper recovers the topology in 10 out of 25 tests. Furthermore, if we replace DBSCAN with HDBSCAN, density-based Mapper performs even better, with correct output in 19 out of 25 tests (Figure 8). This is in contrast with regular Mapper, which performs

much worse with HDBSCAN; we could not get Mapper to recover the correct topology with HDBSCAN for any choice of parameters. Code to reproduce these tests is in Appendix A.

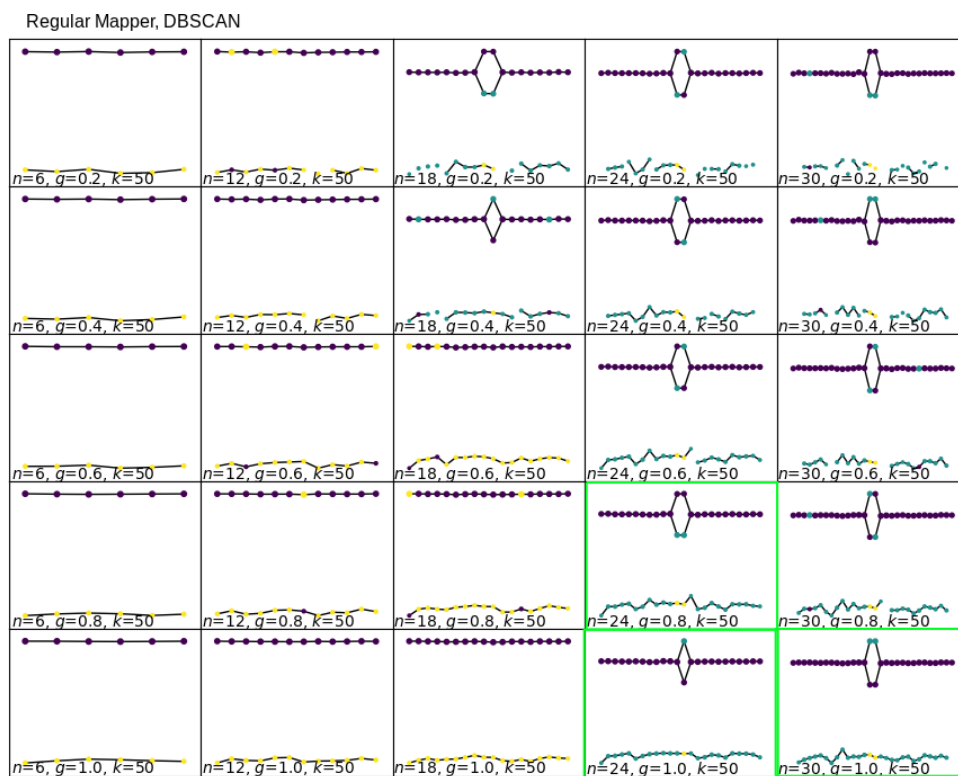


Figure 6: Mapper outputs for a range of parameter choices, with DBSCAN clustering.

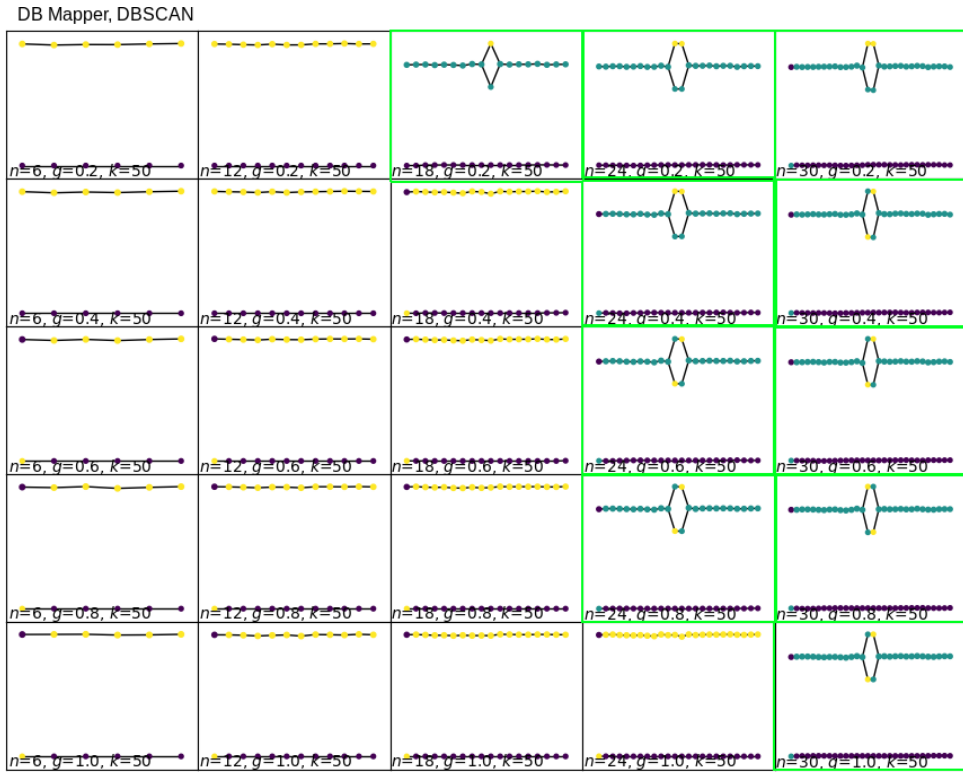


Figure 7: DBMapper outputs for a range of parameter choices, with DBSCAN clustering.

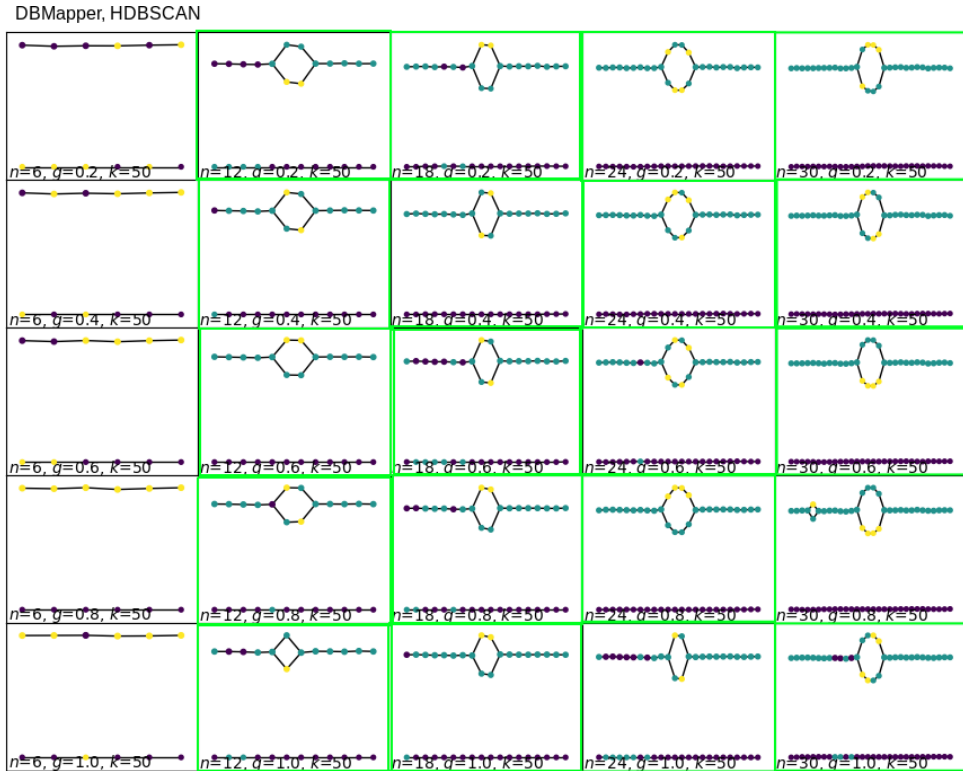


Figure 8: DBMapper outputs for a range of parameter choices, with HDBSCAN clustering.

These figures also demonstrate the failure modes of Mapper and DBMapper. Mapper can fail to find topological components, such as on the left side of all three figures, where the output is missing the 1-dimensional component of the dataset. Mapper can also find spurious topological components, such as the top-right of Figure 6, where there are many extra connected components, or for $n = 30, g = 0.8$ in Figure 8, where there is an extra 1-dimensional component.

6 Conclusions and Future Research

Here we provide the key conclusions of this work, and our suggestions for promising future research, both theoretical and applied.

6.1 Conclusions

By varying the resolution parameter of Mapper with semantic space co-ordinates, one can generate more accurate Mapper graphs. This variation can be done according to density of samples in the image of the Morse function, avoiding the need for additional parameterization choices. These improvements should make Mapper more robust for data analysis in situations where there is large variation in lens-space density across the dataset, and ease parameter selection for Mapper for complex datasets in general.

Consider for example, research papers embedded using a neural network into \mathbb{R}^d , with their time of publication added as a $d + 1^{\text{th}}$ component. Using projection to the time axis as a Morse-type function, different semantic areas in the document embedding space may have different rates of publication, that is, different lens-space density. Our approach allows Mapper to provide more consistent and reasonable output in this situation.

We verified the correctness of our proposal with a mathematical proof that density-based Mapper captures at least all of the topological features that Mapper does, with the same parameters. Furthermore, we tested our reference implementation on some test data that Mapper struggles with, giving preliminary computational evidence for our proposal’s efficacy.

In addition to this article, we have released a reference implementation which is geared towards application to temporal topic modelling, accessible at:

<https://github.com/tutteinstitute/temporal-mapper>.

6.2 Future Research

On the theory side, there are some remaining questions of interest. Recently, it was shown that every graph is a Mapper graph if you permit changing the Morse-type function f (Alvarado et al., 2024). Our work suggests that for a fixed f , there may be graphs which are not Mapper graphs, but are density-based Mapper graphs. It would be interesting to find an example, or a construction of Mapper parameters with fixed f for any given density-based Mapper graph.

Furthermore, when using a clustering algorithm that permits weighting the input points, the shape of kernel used in density-based Mapper has some effect on the output graph, and this effect is not well-understood. More research is required to understand this relationship, and to determine the practical trade-offs of using different kernel shapes.

Finally, for datasets $\mathbb{X}_n \subset X$ whose points are uniformly distributed in $L = f(X)$, density-based Mapper reduces to regular Mapper. Thus, it may be possible to prove that density-based Mapper is equivalent to a composition of a uniformization process similar to UMAP followed by Mapper. If this turns out to be true, it may suggest a natural way to generalize density-based Mapper to d -dimensional lens functions.

On the application side, we are interested in combining our work with other efforts to robustify Mapper. In particular, G -Mapper (Alvarado et al., 2023) provides a method for selecting the resolution r . We suspect that using their method to select an initial resolution,

then varying it according to lens-space density, will be a highly effective way of choosing Mapper parameters.

The initial motivation for this project came from *temporal topic modelling*, which means trying to understand how topics in a corpus of documents change over time. Using time as a Morse-type function, a Mapper graph can be interpreted in terms of birth, death, merging and splitting of topics over time. We hope to apply the method introduced here to some real-world temporal modelling problems, which are likely to introduce further complications to be solved.

References

- Enrique Alvarado, Robin Belton, Emily Fischer, Kang-Ju Lee, Sourabh Palande, Sarah Percival, and Emilie Purvine. G-Mapper: Learning a Cover in the Mapper Construction, 2023. URL <https://arxiv.org/abs/2309.06634>.
- Enrique G. Alvarado, Robin Belton, Kang-Ju Lee, Sourabh Palande, Sarah Percival, Emilie Purvine, and Sarah Tymochko. Any Graph is a Mapper Graph, August 2024. URL <http://arxiv.org/abs/2408.11180>. arXiv:2408.11180 [cs, math].
- Quang-Thinh Bui, Bay Vo, Hoang-Anh Nguyen Do, Nguyen Quoc Viet Hung, and Vaclav Snasel. F-Mapper: A Fuzzy Mapper clustering algorithm. *Knowledge-Based Systems*, 189: 105107, February 2020. ISSN 0950-7051. doi: 10.1016/j.knosys.2019.105107. URL <https://www.sciencedirect.com/science/article/pii/S0950705119304794>.
- Gunnar Carlsson and Vin de Silva. Zigzag Persistence, November 2008. URL <http://arxiv.org/abs/0812.0197>. arXiv:0812.0197 [cs].
- Gunnar Carlsson, Vin De Silva, and Dmitriy Morozov. Zigzag persistent homology and real-valued functions. In *Proceedings of the twenty-fifth annual symposium on Computational geometry*, pages 247–256, Aarhus Denmark, June 2009. ACM. ISBN 978-1-60558-501-7. doi: 10.1145/1542362.1542408. URL <https://dl.acm.org/doi/10.1145/1542362.1542408>.
- Mathieu Carriere, Bertrand Michel, and Steve Y. Oudot. Statistical analysis and parameter selection for Mapper. *Journal of Machine Learning Research*, 2018. URL <https://hal.science/hal-01633106>.
- Mathieu Carrière and Steve Oudot. Structure and Stability of the 1-Dimensional Mapper. *Foundations of Computational Mathematics*, 18(6):1333–1396, December 2018. ISSN 1615-3375, 1615-3383. doi: 10.1007/s10208-017-9370-z. URL <http://arxiv.org/abs/1511.05823>. arXiv:1511.05823 [cs, math].
- Bishal Deb, Ankita Sarkar, Nupur Kumari, Akash Rupela, Piyush Gupta, and Balaji Krishnamurthy. Multimapper: Data Density Sensitive Topological Visualization. In *2018 IEEE International Conference on Data Mining Workshops (ICDMW)*, pages 1054–1061, Singapore, Singapore, November 2018. IEEE. ISBN 978-1-5386-9288-2. doi: 10.1109/ICDMW.2018.00153. URL <https://ieeexplore.ieee.org/document/8637470/>.
- Tamal K. Dey and Yusu Wang. Reeb Graphs: Approximation and Persistence. *Discrete & Computational Geometry*, 49(1):46–73, January 2013. ISSN 1432-0444. doi: 10.1007/s00454-012-9463-z. URL <https://doi.org/10.1007/s00454-012-9463-z>.
- Gurjeet Singh, Facundo Memoli, and Gunnar Carlsson. Topological Methods for the Analysis of High Dimensional Data Sets and 3D Object Recognition. *Eurographics Symposium on Point-Based Graphics*, page 10 pages, 2007. ISSN 1811-7813. doi: 10.2312/SPBG/SPBG07/091-100. URL <http://diglib.eg.org/handle/10.2312/SPBG.SPBG07.091-100>.

Appendix A. Code to Reproduce Computational Experiments.

In this appendix we've included python 3 code snippets which can be used to reproduce the computational experiments described in Section 5.

A.1 Synthetic Data Generation

The code in this section was used to generate the synthetic data in the experiments. A working environment should require only python 3, and recent versions of numpy and matplotlib.

The following code block generates Figure 3.

```
1 import numpy as np
2 from numpy.random import randn
3 import matplotlib.pyplot as plt
4
5 def generate_consistent(n_pts, loc, width):
6     x,y=loc
7     widthx,widthy=width
8     x_axis = widthx * np.random.randn(n_pts,) + x
9     y_axis = widthy * np.random.randn(n_pts,) + y
10    t_axis = 10*np.random.rand(n_pts,)
11
12    cluster_consistent = np.array([
13        x_axis,
14        y_axis,
15        t_axis,
16    ])
17    return cluster_consistent.T
18
19 d1 = generate_consistent(200, (3,0), (0.3,0.2))
20 d2 = generate_consistent(600, (0,0), (0.3,0.2))
21 d3 = generate_consistent(1800, (-3,0), (0.3,0.2))
22
23 cluster_merge = np.concatenate((d1,d2,d3),axis=0)
24 cluster_merge = np.squeeze(cluster_merge)
25 intended_clusters = [0]*200 + [1]*600 + [2]*1800
26
27 fig = plt.figure()
28 ax = fig.add_subplot(projection='3d')
29 ax.scatter(
30     cluster_merge[:,0],
31     cluster_merge[:,1],
32     cluster_merge[:,2],
33     c=intended_clusters
34 )
35 ax.set_ylim(-5,5)
36 ax.set_xlim(-5,5)
37 ax.set_zlim(0,10)
38 plt.show()
39 np.save("./density_demo_data.npy",cluster_merge)
```

The following code block generates Figure 5.

```
1 import numpy as np
2 from numpy.random import randn
3 import matplotlib.pyplot as plt
4
5 angles = np.random.randn(2000,)
6 circle = np.array([
7     0.6*np.cos(2*np.pi*angles), 1.2*np.sin(2*np.pi*angles)+2
8 ])
9 circle += 0.1*np.random.randn(2000,2)
```



```

10 left=np.amin(circle[:,0])+0.13
11 right=np.amax(circle[:,0])-0.13
12 handle_leftx = np.linspace(-3,left,2500)+ 0.1*np.random.randn(2500,)
13 handle_rightx = np.linspace(right,3,2500)+ 0.1*np.random.randn(2500,)
14 handle_x = np.hstack((handle_leftx,handle_rightx))
15 handle = np.array([
16     handle_x, 0.3*np.random.randn(5000,)+2
17 ]).T
18 dense = np.vstack((handle, circle))
19
20 sparse_x = np.linspace(-3,3,200)
21 sparse_x += 0.1*np.random.randn(200,)
22 sparse = np.array([
23     sparse_x, 0.5*np.random.randn(200,)-3
24 ]).T
25
26 points = np.vstack((dense, sparse))
27 np.save("./genus1_demo.npy",points)
28
29 fig, ax = plt.subplots(1)
30 ax.set_title("Experiment 1 Generated Data")
31 ax.scatter(
32     points[:,0], points[:,1],
33     marker='.',
34     s=1,
35 )
36 ax.set_xlabel(r'$T$')
37 ax.set_ylabel(r'Semantic space ( $\mathbb{R}^n$ )')
38 plt.savefig("./e1_data.png")
39 plt.show(fig)

```

A.2 Running the Reference Implementation

Here we provide code snippets used to run our reference implementation of DBMapper in the experiments. The reference implementation can be downloaded from GitHub, at [\(link here\)](#). For this article, the version used is v 0.4.0, which can be obtained from the Releases section of the GitHub page.

The following code block generates Figure 4.

```

1 import numpy as np
2 import pandas as pd
3 import datamapplot
4 import sys
5 import os
6 import networkx as nx
7 import temporalmapper as tm
8 import temporalmapper.utilities_ as tmutils
9 import temporalmapper.weighted_clustering as tmwc
10
11 import matplotlib.pyplot as plt
12 from matplotlib.colors import to_rgb
13 from sklearn.decomposition import PCA
14 from sklearn.neighbors import NearestNeighbors
15 from mpl_toolkits.axes_grid1 import make_axes_locatable
16 from sklearn.metrics import pairwise_distances
17 from sklearn.cluster import DBSCAN
18
19 data_time = np.load("data/density_test_data.npy")
20 data = data_time[:,0:2]
21 time = data_time[:,2]

```

```

22 sorted_indices = np.argsort(time)
23 time = time[sorted_indices]
24 data = data[sorted_indices]
25 N_data = np.size(time)
26
27
28 # Construct the temporal graph.
29 map_data = data
30 y_data = PCA(n_components=1).fit_transform(data)
31 clusterer = DBSCAN()
32 N_checkpoints = 20
33 kernel_params = (1),
34 TG = tm.TemporalMapper(
35     time,
36     map_data,
37     clusterer,
38     N_checkpoints = N_checkpoints,
39     neighbours = 150,
40     slice_method='time',
41     overlap=1,
42     rate_sensitivity=1,
43     kernel=tmwc.square,
44     verbose=True
45 )
46 TG.build()
47
48 idx=15
49 slice_ = (TG.weights[idx] >= 0.1).nonzero()
50 cp_with_ends = [np.amin(time)]+list(TG.checkpoints)+[np.amax(time)]
51 bin_width = (cp_with_ends[idx+1]-cp_with_ends[idx])
52 fig, (ax1,ax2) = plt.subplots(1,2)
53 fig.set_figwidth(10)
54 ax1.set_title(f"$f$-Density")
55 sca=ax1.scatter(time,y_data,s=1,c=TG.density)
56 ax2.scatter(time,y_data,s=1,c='grey')
57 divider = make_axes_locatable(ax1)
58 cax = divider.append_axes('right', size='5%', pad=0.05)
59 fig.colorbar(sca, cax=cax, orientation='vertical')
60 ax2.scatter(time[slice_],y_data[slice_],s=1,c='red')
61 tstr = f'Pullback of $({TG.checkpoints[idx]}-(bin_width/2)*(1+TG.g):.2f),{TG.
    checkpoints[idx]+bin_width/2*(1+TG.g):.2f})$'
62 ax2.set_title(tstr)
63 ax2.set_xlabel("Time")
64 ax1.set_xlabel("Time")
65 ax1.set_ylabel("PCA to 1d")
66 ax2.axvline(TG.checkpoints[idx]+(bin_width/2)*(1+TG.g),c='k')
67 ax2.axvline(TG.checkpoints[idx]-(bin_width/2)*(1+TG.g),c='k')
68 plt.savefig("td-verify.png")
69 plt.show()

```

The following code block generates Figures 6-8.

```

1 import numpy as np
2 import pandas as pd
3 import datamaplot
4 import sys
5 import os
6 import networkx as nx
7 import temporalmapper as tm
8 import temporalmapper.utilities_ as tutils
9 import temporalmapper.weighted_clustering as tmwc
10 import matplotlib.pyplot as plt

```

```

11 from matplotlib.colors import to_rgb
12 from sklearn.decomposition import PCA
13 from sklearn.neighbors import NearestNeighbors
14 from sklearn.cluster import DBSCAN
15 from mpl_toolkits.axes_grid1 import make_axes_locatable
16 import matplotlib as mpl
17 from tqdm import trange
18
19 data_time = np.load("data/genus1_demo.npy")
20 data_unsort = data_time[:,1].T
21 timestamps_unsort = data_time[:,0].T
22 sorted_indices = np.argsort(timestamps_unsort)
23 data = data_unsort[sorted_indices]
24 timestamps = timestamps_unsort[sorted_indices]
25 N_data = np.size(timestamps)
26 map_data = y_data = data
27
28 def generate_plot(TG, label_edges = True, ax=None, threshold = 0.2, vertices =
None):
29     self = TG
30     if ax is None:
31         ax = plt.gca()
32     if type(vertices) == type(None):
33         vertices = self.G.nodes()
34
35     G = self.G.subgraph(vertices)
36     pos = {}
37     slice_no = nx.get_node_attributes(TG.G, 'slice_no')
38     for node in vertices:
39         t = slice_no[node]
40         pt_idx = TG.get_vertex_data(node)
41         w = TG.weights[t,pt_idx]
42         node_ypos = np.average(np.squeeze(TG.data[pt_idx]), weights=w)
43         node_xpos = t #np.average(TG.time[pt_idx], weights=w)
44         pos[node] = (node_xpos, node_ypos)
45
46     edge_width = np.array([d["weight"] for (u,v,d) in G.edges(data = True)])
47     elarge = [(u, v) for (u, v, d) in G.edges(data=True) if d["weight"] >=
threshold]
48     esmall = [(u, v) for (u, v, d) in G.edges(data=True) if 0.1 < d["weight"] <
threshold]
49     nx.draw_networkx_edges(G, pos, ax=ax, edgelist=elarge, width=1, arrows=
False)
50     if label_edges:
51         edge_labels = nx.get_edge_attributes(G, "weight")
52         nx.draw_networkx_edge_labels(G, pos, edge_labels)
53
54     node_size = [np.log2(np.size(self.get_vertex_data(node))) for node in
vertices]
55     clr_dict = nx.get_node_attributes(self.G, 'cluster_no')
56     node_clr = [clr_dict[node] for node in vertices]
57
58     nx.draw_networkx_nodes(G, pos, ax=ax, node_size=node_size, node_color=
node_clr)
59     return ax
60
61 """
62 Running standard mapper over a range of parameters, with DBSCAN.
63 """
64
65 checkpoint_numbers = [6,12,18,24,30]

```

```

66 overlap_parameters = [0.2,0.4,0.6,0.8,1.]
67
68 fig, axes = plt.subplots(5,5)
69 fig.set_figwidth(11)
70 fig.set_figheight(8.5)
71 fig.dpi = 200
72 axes = axes.reshape(5*5)
73 clusterer = DBSCAN()
74 j = 0
75 for k in trange(25):
76     TG = tm.TemporalMapper(
77         timestamps,
78         map_data,
79         clusterer,
80         N_checkpoints = checkpoint_numbers[k%5],
81         neighbours = 50,
82         overlap = overlap_parameters[j],
83         slice_method='time',
84         rate_sensitivity=0,
85         kernel=tmwc.square,
86         #kernel_params=(overlap_parameters[j],),
87     )
88     TG.build()
89     generate_plot(TG,label_edges = False,ax=axes[k])
90     xmin,xmax=axes[k].get_xlim()
91     ymin,ymax=axes[k].get_ylim()
92     axes[k].text(xmin+0.1,ymin+0.1,fr'$n$={TG.N_checkpoints}, $g$={TG.g}, $k$
    ={50}')
93     if k%5==4:
94         j+=1
95 plt.subplots_adjust(wspace=0, hspace=0)
96 plt.savefig("genus1-regular-dbscan.png")
97 plt.show()
98
99 """
100 Running fuzzy mapper over a range of parameters, with DBSCAN.
101 """
102 checkpoint_numbers = [6,12,18,24,30]
103 overlap_parameters = [0.2,0.4,0.6,0.8,1.]
104
105 fig, axes = plt.subplots(5,5)
106 fig.set_figwidth(11)
107 fig.set_figheight(8.5)
108 fig.dpi = 200
109 axes = axes.reshape(5*5)
110 clusterer = DBSCAN()
111 j = 0
112 for k in trange(25):
113     TG = tm.TemporalMapper(
114         timestamps,
115         map_data,
116         clusterer,
117         N_checkpoints = checkpoint_numbers[k%5],
118         neighbours = 50,
119         slice_method='time',
120         overlap = overlap_parameters[j],
121         rate_sensitivity=1,
122         kernel=tmwc.square,
123     )
124     TG.build()
125     generate_plot(TG,label_edges = False,ax=axes[k])

```

```

126     xmin, xmax=axes[k].get_xlim()
127     ymin, ymax=axes[k].get_ylim()
128     axes[k].text(xmin+0.1, ymin+0.1, fr'$n$={checkpoint_numbers[k%5]}, $g$={
overlap_parameters[j]}, $k$={50}')
129     if k%5==4:
130         j+=1
131 plt.subplots_adjust(wspace=0, hspace=0)
132 plt.savefig("genus1-db-dbscan.png")
133 plt.show()
134
135 """
136 Running fuzzy mapper over a range of parameters, with HDBSCAN.
137 """
138 checkpoint_numbers = [6,12,18,24,30]
139 overlap_parameters = [0.2,0.4,0.6,0.8,1.]
140
141 fig, axes = plt.subplots(5,5)
142 fig.set_figwidth(11)
143 fig.set_figheight(8.5)
144 fig.dpi = 200
145 axes = axes.reshape(5*5)
146 clusterer = HDBSCAN(min_cluster_size=50)
147 j = 0
148 for k in trange(25):
149     TG = tm.TemporalMapper(
150         timestamps,
151         map_data,
152         clusterer,
153         N_checkpoints = checkpoint_numbers[k%5],
154         neighbours = 50,
155         slice_method='time',
156         overlap = overlap_parameters[j],
157         rate_sensitivity=1,
158         kernel=tmwc.square,
159     )
160     TG.build()
161     generate_plot(TG, label_edges = False, ax=axes[k])
162     xmin, xmax=axes[k].get_xlim()
163     ymin, ymax=axes[k].get_ylim()
164     axes[k].text(xmin+0.1, ymin+0.1, fr'$n$={checkpoint_numbers[k%5]}, $g$={
overlap_parameters[j]}, $k$={50}')
165     if k%5==4:
166         j+=1
167 plt.subplots_adjust(wspace=0, hspace=0)
168 plt.savefig("genus1-db-hdbscan.png")
169 plt.show()

```